UNIVERSITY of York

This is a repository copy of *Impurity band assisted carrier relaxation in Cr doped topological insulator Bi2Se3*.

White Rose Research Online URL for this paper:
https://eprints.whiterose.ac.uk/173538/

Version: Accepted Version

Article:
Tu, Jian, Zhao, Yafei, Zhang, Xiaoqian et al. (14 more authors) (2021) Impurity band assisted carrier relaxation in Cr doped topological insulator Bi2Se3. Applied Physics Letters. 081103. ISSN 0003-6951

https://doi.org/10.1063/5.0039440

Reuse
Items deposited in White Rose Research Online are protected by copyright, with all rights reserved unless indicated otherwise. They may be downloaded and/or printed for private study, or other acts as permitted by national copyright laws. The publisher or other rights holders may allow further reproduction and re-use of the full text version. This is indicated by the licence information on the White Rose Research Online record for the item.

Takedown
If you consider content in White Rose Research Online to be in breach of UK law, please notify us by emailing eprints@whiterose.ac.uk including the URL of the record and the reason for the withdrawal request.

White Rose
university consortium
Universities of Leeds, Sheffield & York

eprints@whiterose.ac.uk
https://eprints.whiterose.ac.uk/

Impurity band assisted carrier relaxation in Cr doped topological insulator Bi_2Se_3

Jian Tu[1,a], Yafei Zhao[1,a,*], Xiaoqian Zhang[1], Zhonghui Nie[2],Yao Li[1], Yilin Zhang[1], Ion Cristian Edmond Turcu[1], Luca Poletto[3], Xuezhong Ruan[1], Wenqing Liu[1,4],Yu Zhang[5], Rong Zhang[1], Yongbing Xu[1,6]* and Liang He[1,*]

[1]Jiangsu Provincial Key Laboratory of Advanced Photonic and Electronic Materials, School of Electronic Science and Engineering and Collaborative Innovation Center of Advanced Microstructures, Nanjing University, Nanjing 210093, China

[2]MIIT Key Laboratory of Advanced Display Materials and Devices, Institute of Optoelectronics & Nanomaterials, College of Materials Science and Engineering, Nanjing University of Science and Technology, Nanjing 210094, China

[3]National Research Council Institute of Photonics and Nanotechnologies, Padova 35131, Italy

[4]Department of Electronic Engineering, Royal Holloway University of London, Egham TW20 0EX, UK

[5]Central Laser Facility, STFC Rutherford Appleton Laboratory, Didcot OX11 0QX, United Kingdom.

[6]York-Nanjing Joint Center in Spintronics, Department of Electronic Engineering, the University of York, York, YO10 5DD, United Kingdom.

[a]These authors contributed equally to this work.

E-mail:heliang@nju.edu.cn; njnjzhao@nju.edu.cn; ybxu@nju.edu.cn

Abstract

Topological insulators (TIs) with unique band structures have wide application prospects in the fields of ultra-fast optical and spintronic devices. The dynamics of hot carriers plays a key role in these TI based devices. In this work, using time and angle resolved photoemission spectroscopy (TR-ARPES) technique, the relaxation process of the hot carriers in Cr doped Bi_2Se_3 has been systematically studied, where the ferromagnetic TI is one of the key building blocks for the next generation spintronics. It is found that the electronic temperature (T_e) and chemical potential (μ) decrease faster with the increase of the Cr doping concentration. Similarly, the lifetime (τ) of the excited electrons also decreases with more Cr doped into TIs. The results suggest a new mechanism of the impurity bands assisted carrier relaxation, where the impurity bands within the bulk band gap introduced by Cr doping provide significant recombination channels for the excited electrons. This work directly illustrates the dynamic process of the carriers in Cr doped Bi_2Se_3, which is expected to promote the applications of $(Bi_{1-x}Cr_x)_2Se_3$ in ultrafast optical and spintronic devices.

Keywords: TR-ARPES, Cr doped Bi_2Se_3, hot carriers, ultrafast optical and spintronic devices.

TIs are a class of quantum materials featuring with a bandgap in its bulk and unique Dirac-like metallic states on the surface, which have abroad application prospects in the fields of ultrafast optical and spintronic devices[1-3]. The performance of these devices depends on the dynamics of the hot carriers in TIs, which can be observed directly by TR-ARPES[4-6]. So far, a number of works have been carried on illustrating the recovery process of the excited electrons in TIs due to various mechanisms: such as the phonons assisted,[7,8] the surface states assisted,[9] and the electron-electron scattering assisted.[10,11]

Recently, numerous work have reported that the doping with transition metals can introduce novel physical phenomena in TIs, such as quantum anomalous Hall effect (QAHE)[12], the giant magneto-optical Kerr effect[13], and chiral Majorana fermions[14]. In addition, the doping with transition metals changes the band structure of TIs by weakening the surface state and increasing the bulk bandgap. This suggests that it may also affect the carrier relaxation. However, this has not been systematically studied experimentally, though it is crucial to the application of TIs in the field of ultrafast optical and spintronic devices.

In this work, a series of $(Bi_{1-x}Cr_x)_2Se_3$ (x = 0 ~ 0.074) samples were grown by molecular beam epitaxy (MBE). Then, the dynamic processes of the excited electrons in $(Bi_{1-x}Cr_x)_2Se_3$ are directly studied by the TR-ARPES. It is found that as the Cr doping concentration increases, the relaxation rate of T_e and μ increase, and τ of the excited electrons decreases. This has been attributed to the mechanism of the impurity bands

assisted carrier relaxation. The impurity bands within the bulk band gap introduced by Cr provide more recombination channels for the excited electrons. This provides direct insight into the relaxation mechanisms of the Cr doped TIs, and therefore has profound implications for future works exploring the potential of these materials for ultrafast optical and spintronic devices.

Results

The Bi_2Se_3 and $(Bi_{1-x}Cr_x)_2Se_3$ ultrathin films are grown on fluorophlogopite [$KMg_3(AlSi_3O_{10})F_3$] substrates by MBE. Compared with conventional epitaxy, van der Waals epitaxy (VDW) growth significantly relaxes the stringent conditions of lattice match between the substrate and the epitaxial layer[15-17]. And, atomically flat fluorophlogopite with pseudohexagonal layered structure is suitable for VDW epitaxy growth of layered material due to no dangling bonds associated with the surface[18,19]. The Cr dopants are evaporated simultaneously with the Bi and Se atoms and deposited on fluorophlogopite at 200°C. The growth was carried out under the Se-rich environment with a nominal Se to Bi ratio of 20:1, which is beneficial to reduce the Se vacancy defects[20]. The Cr doping concentration (x= 0.013~0.074) is determined by the Cr deposition flux and the X-ray photoelectron spectroscopy (XPS). Samples were transferred into ARPES chamber through a high vacuum tube ($<3.0\times10^{-9}$ mbar) to ensure the clean surfaces. The band structure of the $(Bi_{1-x}Cr_x)_2Se_3$ films measured by static ARPES (He-I, 21.2eV) at room temperature is shown in Figure 1. It is found that the BVB, surface state and BCB can be clearly distinguished in undoped Bi_2Se_3.

However, the surface state decreases and the bulk band gap increases with the increase of Cr doping concentration. When the Cr doping concentration is increased to x= 0.074, the surface states cannot be observed at all in the band structure. This is consistent with the previous results[21,22].

TR-ARPES measurements were performed using a pump-probe scheme. The laser pulse with 800 nm (~1.55 eV) wavelength and 1 kHz repetition is split into two beams. One beam is used as the pump light to stimulate the sample, and the other is used for high harmonic generation (HHG)[23,24], and the 13th harmonic extreme ultraviolet (EUV) at ~20.15 eV has been chosen as the probe light[25]. Detailed description of the HHG system will be found in our previous work[26]. The overall energy resolution is 190 meV and time resolution is 60 fs. Pump light is *s* polarized, which was maintained at 0.21 mJ/cm^2 during the measurement. Probe pulse is *p* polarized, and the flux of probe pulse is chosen to minimize the space charge effect. All the experiments were carried out at room temperature.

Figure 2(a)-(c) demonstrates the various differential band structures after pumping of Cr (x= 0.013) doped Bi_2Se_3 obtained by EUV by subtracting the un-excited band structure at -0.2 ps. The red and blue represents the increased or decreased electrons at different *E-K* positions. It's found that the intensity above the Fermi level is strongest at 0.7 ps because of the thermalization of the electrons after inelastic scattering process[27]. Then, it starts to reduce at 1.5 ps due to the recombination of excited electrons and holes assisted by phonons. The band structure recovers to un-excited state at 8 ps.

Figure 2e-2g and Figure 2i-2k are the differential band structures of the higher doped samples with x= 0.056 and 0.074, respectively. The similar dynamic process of excited electrons could be seen in these three samples. Namely, after the pump light of 0.7 ps, electrons are excited above the Fermi level, then quickly fall back around the Fermi level, and finally return to its original state[8].

The relaxation dynamics of the hot electrons around the Fermi level after pumping can be quantified by the Fermi-Dirac (FD) distribution convoluted with a Gauss distribution, which considers the energy resolution of the TR-ARPES system:

$$\mathrm{I(E,t)} = A(\mathrm{t}) \int_{-\infty}^{\infty} [F(\varepsilon, T_e(t), \mu(t)) D(\varepsilon)] G(E-\varepsilon, \sigma)] d\varepsilon \quad (1)$$

Here, I represent the energy dispersion curve (EDC) as a function of time delay, F is the FD distribution, T_e and μ denote the electron temperature and chemical potential of the electrons. G is the Gauss distribution to take the overall energy resolution of the system (mainly depending on EUV) into account. A and D are the scale factor[28] and the product of photoemission matrix element and the density of state, respectively[29]. Due to the complexity to determine the D[30], in the fitting process, a narrow range around the Γ point ($\pm$ 0.01 $\mathrm{Å}^{-1}$ around the center) has been used to extract the leading edge of the EDCs (as shown in Figure 2d, 2h and 2l). With this way, D can be treated as a constant. Although this simple treatment neglects the fine structure in D, it is helpful to compare the dynamic process of different samples quantitatively.

Figure 2(d) demonstrates EDCs of x= 0.013 at the different delay time. It is found that the EDC at 0.7 ps (black line) shifts to the higher energy compared to -0.2 ps (red

line), which means the T_e and μ of the former are higher. This is due to the thermalization of electrons in CB after absorbing the energy from pumps photons. The EDC at 1.5ps shows intermediate features compared with above two due to the energy exchange between exited electrons and phonons help the relaxation of electrons. At 8 ps after the arrival of pump photons, the excited electrons almost recombine with the holes and the sample recovers to the state before excited. EDCs at the same delay time of x=0.056 (Figure 2h) and 0.074 (Figure 2l) showed a similar recovery process.

Moreover, T_e and μ as a function of delay time with different x were extracted using Eq. (1) to fit the EDCs, as shown in Figure 3a and 3b. The T_e of x= 0 reveal a quick relaxation from the peak value to around 500~590 K, and maintain around that temperature within the detection window (Figure 3a). The reason is that the weak coupling of phonons and surface electrons. It should be noted that the $\Delta\mu$ versus delay time does not satisfy exponential decay function at low Cr doping concentration, suggesting that the activity of phonons at the surface of pure Bi_2Se_3 is weak[31]. Interestingly, with the increase of x (x= 0.013~0.074), T_e and $\Delta\mu$ recover to the state before pump pulse more quickly, which also demonstrate the ability of Cr doping to assist the relaxation of excited electrons.

In order to reveal the τ of the excited carriers, a black box was fixed at 0.1 eV above the Fermi level (as shown in Figure 2a) to indicate the integral domain. The integral intensities as a function of pump-probe delay time for various $(Bi_{1-x}Cr_x)_2Se_3$ films are shown in Figure 3c. After pumping light, electrons are immediately excited

above the Fermi level, and then quickly fall back around the Fermi level[32]. After that, electrons relax to its original state facilitated by electron-phonon scattering process[8]. Thus, the excited electrons have the same recovery tendency as T_e and $\Delta\mu$. Meanwhile, the electron relaxation rate of undoped Bi_2Se_3 is slower than that of Cr doped Bi_2Se_3. Namely, the Cr doping reduces the τ of excited electrons. By use of single exponential decay function to fit the curves in Figure 3c, the τ of excited electrons can be extracted as a function of x, as shown in Figure 3d. It is found that τ decreases monotonically with the increase of doping concentrations x.

Discussion

Two factors have been reported to influence the τ of the excited electrons in TIs[4,7]. First, the existing of surface state, which provides additional paths (2 and 3) for the electrons through the coupling of TSS and BCB (Figure 4a) [4], helps the relaxation of excited electrons. Thus, higher Cr doped samples should have longer τ, because of the disappearing of the TSS[33]. Second, doping Cr enlarges the bulk bandgap as shown in Figure 3d, which are extracted by a multi-peaks Gaussian fitting around the Γ point in Figure 1. And this is consistent with our calculated band structure by VASP package (Supporting Information Figure S1). However, the reports demonstrate that the enlarged bulk band gap can only increase τ of the excited carriers[22], which is again controversy to this work.

To explain our results, we propose here a new mechanism of the impurity band assisted carrier relaxation. The band structures of $(Bi_{1-x}Cr_x)_2Se_3$ have been shown in

Figure S1. It is found that the impurity bands (mainly composed of Cr-*d* states) appear at the bottom of BCB and the top BVB after doping Cr, as shown by the red dashed lines in Figure 4b and Figure S1. Moreover, as more Cr atoms are doped into the lattice, the density of states of impurity bands increases. Due to the existence of impurity band, the excited electrons in the BCB can move to the impurity band through thermal relaxation process. And they then can jump down to the impurity band above the top of the BVB (path 3) or the BVB (path 4), as shown in Figure 4b. Thus, these impurity bands provide additional recombination channels, which assist the relaxation of the exited carriers[34,35].

According to shock-read-Hall recombination theory, considering n-type conduction and low optical injection situation in this work, the recombination rate (R_I) of excess carriers passing through path 2, path 3 and path 4 can be written as: $R_I = (C_2N_I + C_3N_I + C_4N_I)\delta_p$, quantitatively. C_2, C_3 and C_4 are constants representing the hole capture cross-section of impurity bands. δ_p is the number of excess holes, which can be treated as a constant due to the invariable pump power density. N_I is the number of the trap center, and it can be estimated by the integral of the density of states of the impurity band. Meanwhile, the recombination rate of the bulk (path 1) (R_B) can be expressed as: $R_B = C_1N_B\delta_p$. C_1 is a constant representing the hole capture cross-section of CB. N_B is the density of states at the bottom of the conduction band.

Here, τ of the excited carriers is proportional to $1/R$, so it can be written as:

$$\tau = \frac{1}{R_I + R_B} = \frac{1}{(C_2 + C_3 + C_4)N_I + C_1N_B} \tag{2}$$

Because C_1, C_2, C_4 and N_B are constants, τ can be simplified as: $\tau = \frac{1}{C_2' N_I + C_1'}$. As C_2' and C_1' are constants, the τ vs. impurity band density can be fitted by equation 2 as shown in Figure 4c. Here, a background constant τ_0 has been added as: $\tau = \tau_0 + \frac{1}{C_2' N_I + C_1'}$. The fitting results agree well within the experimental data, suggesting that τ of the hot carriers shortens with the increase of the density of states of impurity band. Thus, the impurity bands induced by the Cr doping provide additional recombination paths, overcome the previous two factors, and effectively lower τ of the hot electrons.

Conclusion

In summary, we have systematically studied the dynamic process of photoexcited carriers in high quality $(Bi_{1-x}Cr_x)_2Se_3$ with different Cr doping concentrations by TR-ARPES. It is found that as the Cr doping concentration increases, the T_e and μ decrease faster. Secondly, τ of the excited electrons decreases with the increase of Cr doping concentration. This has been attributed to the new relaxation mechanism that the impurity bands induced by doping provide additional recombination paths, and effectively lower τ of the hot electrons. This work has found that the doping can tune the carrier relaxation in TIs, which may promote their applications in ultrafast optical and spintronic devices.

ACKNOWLEDGEMENTS

This work is supported by the National Key Research and Development Program of China (No. 2016YFA0300803), the National Natural Science Foundation of China

(No. 61974061, 61674079, 61427812), the Natural Science Foundation of Jiangsu Province of China (No. BK20192006), the China Postdoctoral Science Foundation (No. 2019M661787).

Refences

1. Steinberg, H., Gardner, D. R., Lee, Y. S. & Jarillo-Herrero, P. Surface State Transport and Ambipolar Electric Field Effect in Bi_2Se_3 Nanodevices. *Nano Lett.***10,** 5032 (2010).

2. Checkelsky, J. G., Hor, Y. S., Cava, R. J. & Ong, N. P. Bulk Band Gap and Surface State Conduction Observed in Voltage-Tuned Crystals of the Topological Insulator Bi_2Se_3. *Phys. Rev. Lett.***106,** 196801 (2011).

3. McIver, J. W., Hsieh, D., Steinberg, H., Jarillo-Herrero, P. & Gedik, N. Control over topological insulator photocurrents with light polarization. *Nat. Nano***7,** 96 (2011).

4. Sobota, J. A. *et al.* Ultrafast Optical Excitation of a Persistent Surface-State Population in the Topological Insulator Bi_2Se_3. *Phys. Rev. Lett.***108,** 117403 (2012).

5. Sobota, J. A. *et al.* Direct Optical Coupling to an Unoccupied Dirac Surface State in the Topological Insulator Bi_2Se_3. *Phys. Rev. Lett.***111,** 136802 (2013).

6. Neupane, M. *et al.* Gigantic Surface Lifetime of an Intrinsic Topological Insulator. *Phys. Rev. Lett.***115,** 116801 (2015).

7. Wang, Y. H. *et al.* Measurement of Intrinsic Dirac Fermion Cooling on the Surface of the Topological Insulator Bi_2Se_3 Using Time-Resolved and Angle-Resolved Photoemission Spectroscopy. *Phys. Rev. Lett.***109,** 127401 (2012).

8. Sobota, J. A. *et al.* Distinguishing Bulk and Surface Electron-Phonon Coupling in the Topological Insulator Bi_2Se_3 Using Time-Resolved Photoemission Spectroscopy. *Phys. Rev. Lett.***113,** 157401 (2014).

9. Freyse, F., Battiato, M., Yashina, L. V. & Sánchez-Barriga, J. Impact of ultrafast transport on the high-energy states of a photoexcited topological insulator. *Phys. Rev. B***98,** 115132 (2018).

10. Jozwiak, C. *et al.* Spin-polarized surface resonances accompanying topological surface state formation. *Nat. Commun.***7,** 13143 (2016).

11. Cacho, C. *et al.* Momentum-resolved Spin Dynamics of Bulk and Surface Excited States in the Topological Insulator Bi_2Se_3. *Phys. Rev. Lett.***114,** 097401 (2015).

12. Chang, C.-Z. *et al.* Experimental Observation of the Quantum Anomalous Hall Effect in a Magnetic Topological Insulator. *Science***340,** 167-170 (2013).

13. Tse, W. K. & MacDonald, A. H. Giant magneto-optical Kerr effect and universal Faraday effect in thin-film topological insulators. *Phys. Rev. Lett.***105,** 057401 (2010).

14. Qi, X.-L., Hughes, T. L. & Zhang, S.-C. Chiral topological superconductor from the quantum Hall state. *Phys. Rev. B***82,** 184516 (2010).

15. H. Li *et al.* Controlled Synthesis of Topological Insulator Nanoplate Arrays on Mica. *J. Am. Chem. Soc.***134,** 6132 (2012).

16. Chen, K. H. M. *et al.* Van der Waals epitaxy of topological insulator Bi_2Se_3 on single layertransition metal dichalcogenide MoS_2. *Appl. Phys. Lett.***111,** 083106 (2017).

17. Kou, X. F. *et al.* Epitaxial growth of high mobility Bi_2Se_3 thin films on CdS. *Appl. Phys. Lett.* **98,** 242102 (2011).

18. Liu, Y. *et al.* Epitaxial Growth of Ternary Topological Insulator Bi_2Te_2Se 2D Crystals on Mica. *small***13,** 1603572 (2017).

19. Zheng, W. *et al.* Patterning two-dimensional chalcogenide crystals of Bi_2Se_3 and In_2Se_3 and efficient photodetectors. *Nat. Commun.***6,** 6972 (2015).

20. He, L., Kou, X. & Wang, K. L. Review of 3D topological insulator thin-film growth by molecular

beam epitaxy and potential applications. *Phys. Status Solidi RRL***7,** 50– 63 (2013).

21. Liu, M. *et al.* Crossover between Weak Antilocalization and Weak Localization in a Magnetically Doped Topological Insulator. *Phys. Rev. Lett.***108,** 036805 (2012).

22. Brahlek, M. *et al.* Topological-Metal to Band-Insulator Transition in $(Bi_{1-x}In_x)_2Se_3$ Thin Films. *Phys. Rev. Lett.***109,** 186403 (2012).

23. Ojeda, J. *et al.* Harmonium: A pulse preserving source of monochromatic extreme ultraviolet (30–110eV) radiation for ultrafast photoelectron spectroscopy of liquids. *Struct. Dyn.***3,** 023602 (2016).

24. Grazioli, C. *et al.* CITIUS: An infrared-extreme ultraviolet light source for fundamental and applied ultrafast science. *Rev. Sci. Instrum.***85,** 023104 (2014).

25. Seah, M. P. & Dench, W. Quantitative Electron Spectroscopy of Surfaces: A Standard Data Base for Electron Inelastic Mean Free Paths in Solids. *Surf. Interf. Anal.***1,** 2-11 (1979).

26. Nie, Z. *et al.* Spin-ARPES EUV Beamline for Ultrafast Materials Research and Development. *Appl. Sci.***9,** 370 (2019).

27. Gierz, I. *et al.* Tracking Primary Thermalization Events in Graphene with Photoemission at Extreme Time Scales. *Phys. Rev. Lett.***115,** 086803 (2015).

28. Fann, W. S., Storz, R., Tom, H. W. K. & Bokor, J. Direct Measurement of Nonequilibrium Electron-Energy Distributions in Subpicosecond Laser-Heated Gold Films. *Phys. Rev. Lett.***68,** 2834-2837 (1992).

29. Hüfner, S. *Photoelectron spectroscopy: principles and applications*. Springer Science & Business Media (2013).

30. Ishida, Y. *et al.* Non-thermal hot electrons ultrafastly generating hot optical phonons in graphite.

*Sci. Rep.***1,** 64 (2011).

31. Crepaldi, A. *et al.* Evidence of reduced surface electron-phonon scattering in the conduction band of Bi_2Se_3 by nonequilibrium ARPES. *Phys. Rev. B***88,** 121404(R) (2013).
32. Soifer, H. *et al.* Band-Resolved Imaging of Photocurrent in a Topological Insulator. *Phys. Rev. Lett.***122,** 167401 (2019).
33. Wang, Z. *et al.* Dimensional Crossover and Topological Nature of the Thin Films of a Three-Dimensional Topological Insulator by Band Gap Engineering. *Nano Lett.***19,** 4627-4633 (2019).
34. Sumida, K. *et al.* Magnetic-impurity-induced modifications to ultrafast carrier dynamics in the ferromagnetic topological insulators $Sb_{2x}V_xTe_3$. *New J. Phys.***21,** 093006 (2019).
35. Papalazarou, E. *et al.* Unraveling the Dirac fermion dynamics of the bulk-insulating topological system Bi_2Te_2Se. *Phys. Rev. Mater.***2,** 104202 (2018).

Captions:

Figure 1. (Color online) The band structures of a series of $(Bi_{1-x}Cr_x)_2Se_3$ with x from 0 to 0.074. The bulk bandgap increases with the increase of Cr doping concentration, and the surface states gradually disappear.

Figure 2. (Color online) (a)-(c) Differential band structures of $(Bi_{1-x}Cr_x)_2Se_3$ (x=0.013) around Γ point at t= 0.7 ps, 1.5 ps and 8 ps, respectively, which have subtracted the band structure of t= -0.2 ps. (e)-(g) and (i)-(k) are the differential band structures of $(Bi_{1-x}Cr_x)_2Se_3$ with x= 0.056 and 0.074, respectively. (d), (h) and (l) are the EDCs integrated between $\pm$ 0.01 $Å^{-1}$ around Γ point at different delay time with x= 0.013, 0.056 and 0.074, respectively. Using a convoluted Gaussian and Fermi-Dirac distribution function, T_e and $\Delta\mu$ can be extracted.

Figure 3. (Color online) (a) The T_e and (b) the $\Delta\mu$ as a function of the delay time with different x. And, the T_e and $\Delta\mu$ recover more quickly as the increase of Cr doping concentration. (c) Normalized integral intensities within the black boxes in Figure 2a, as a function of the delay time for different samples. (d) The lifetime (τ) of the excited electrons and bulk bandgap as the function of Cr doped concentration (x).

Figure 4. (Color online) Mechanism diagram of the non-equilibrium carrier recombination process of the (a) undoped and (b) Cr doped Bi_2Se_3. The results show that the impurity band can provide additional carrier recombination channels. Green lines represent the surface states. (c) The Carrier's lifetime (τ) as a function of the density of states of impurity band. The results show that the τ of hot carrier reduces with the increase of the density of states of impurity band.

Figure 1

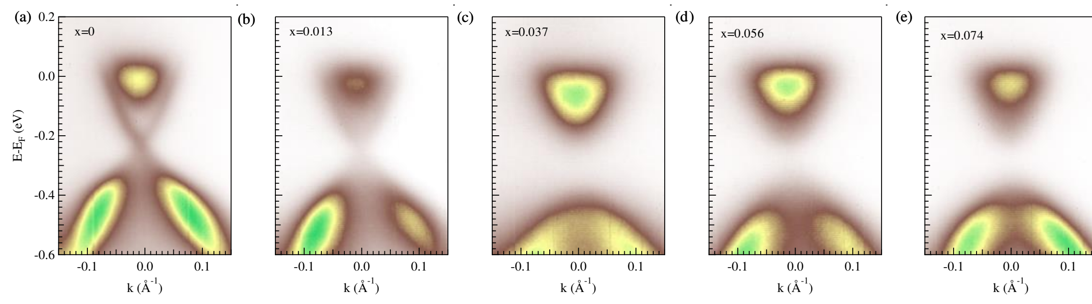

Figure 2

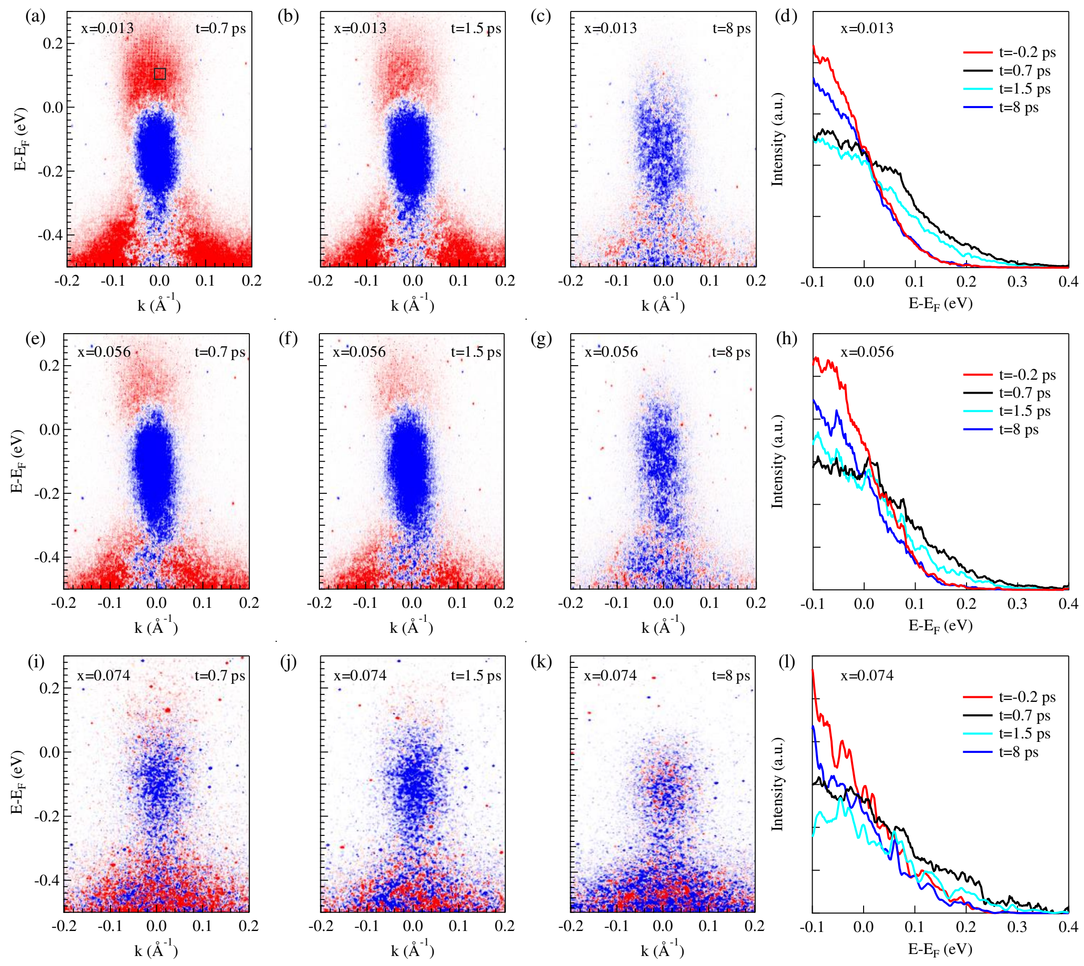

Figure 3

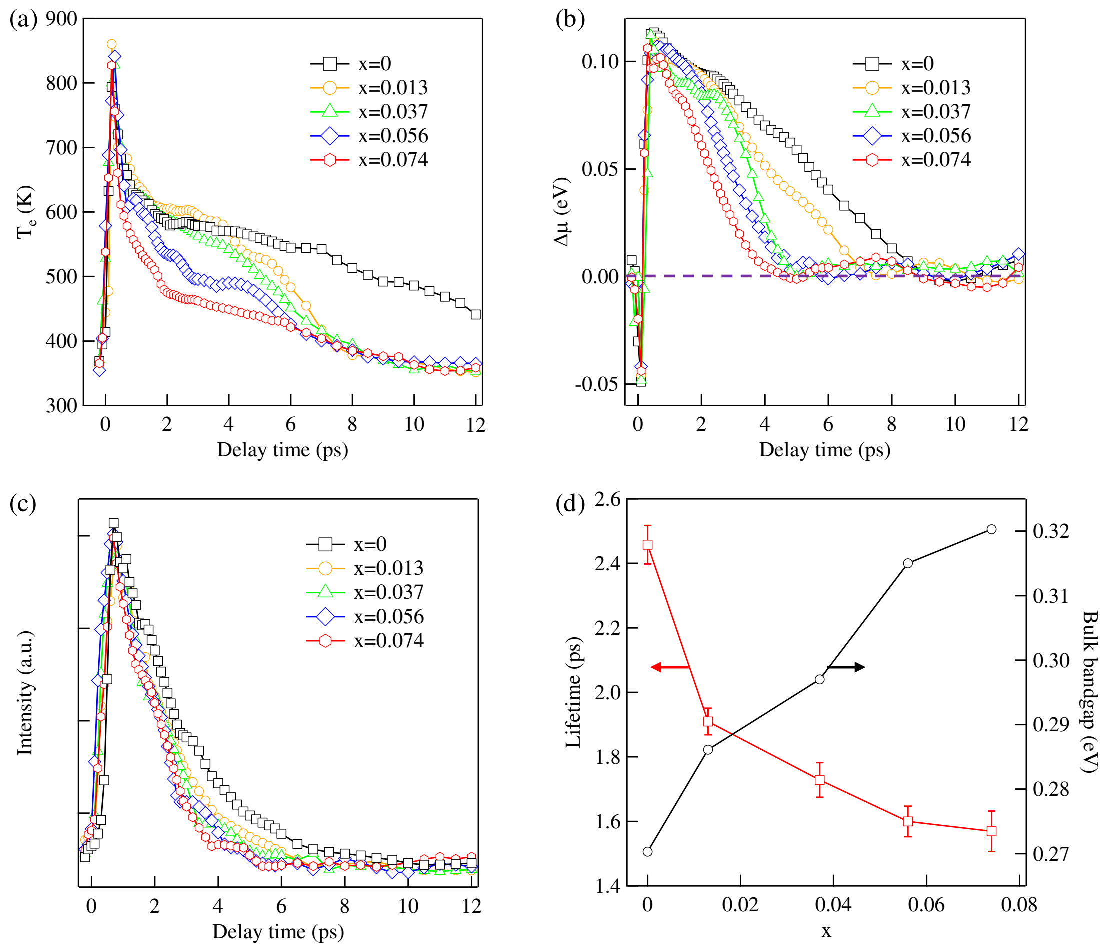

Figure 4